PERGAMON

International Journal of Heat and Mass Transfer 44 (2001) 3973–3984

International Journal of HEAT and MASS TRANSFER

www.elsevier.com/locate/ijhmt

Use of genetic algorithms for the simultaneous estimation of thin films thermal conductivity and contact resistances

S. Orain [a,*], Y. Scudeller [a], S. Garcia [a], T. Brousse [b]

[a] *Laboratoire de Thermocinétique, UMR-CNRS 6607, ISITEM – La Chantrerie, rue Christian Pauc, BP90604, 44306 Nantes cedex 03, France*

[b] *Laboratoire de Génie des Matériaux, ISITEM – La Chantrerie, rue Christian Pauc, BP90604, 44306 Nantes cedex 03, France*

Received 1 October 1999

Abstract

This study is on the use of genetic algorithms (GAs) to develop estimation methodologies for the determination of the thermal properties of thin films. The thermal conductivity and two contact resistances are thought to be simultaneously estimated. A GA is used to minimize a least squares objective function containing calculated and measured temperatures. A photo-thermal technique is applied to acquire measured temperatures, while calculated data are obtained from a one-dimensional conductive model. Experiments were performed on ZrO_2 thin films of different thickness. The results from the analysis demonstrate that the proposed GA is a useful tool for the thermal characterization of thin films. © 2001 Published by Elsevier Science Ltd.

1. Introduction

The development of thin film processing entails considerable needs for thermal characterization. The advanced materials produced this way involve dielectric laying, semi-conductors in electronic, surface treatment of optical components, thermal barrier of combustion fields to name a few. It is common knowledge that the thermal conductivity of a thin film less than 1 μm thick can be much smaller than the property value of the bulk material. This phenomenon is due to structural and microstructural effects that can limit the photons free mean path (defects, impurities, dislocations, grain joints, ...). Techniques for the thermal characterization of these materials are very few. One can mention:

- the photoreflexion methods, which consist of analyzing the reflectivity variation of a metallic film layered on the thin film to be characterized [1,2];
- the methods that involve a thermosensible electrical resistance which is engraved on the thin film to be characterized [3–5].

These methods allow the estimation of an effective thermal conductivity, k_e, which quantifies the global temperature decay between the metal and the substrate. The film conductivity, k, can then be deduced from k_e using an equivalent thermal circuit of the series composite material:

$$k_e^{-1} = k^{-1} + (R_{mf} + R_{fs})e^{-1}, \quad (1)$$

where e is the film thickness and, R_{mf} and R_{fs} are the thermal resistances of the contact metal/film and film/substrate, respectively. These resistances are due to breakings of the crystalline lattice periodicity and existence of both defects (dislocations, gaps, impurities) and components of conductivity interdiffusion in the interfacial zone neighboring. Most of researchers do not take these resistances into account, and more particularly R_{mf}. However, these resistances, which are on the order of 10^{-8}–10^{-7} m^2 K W^{-1}, should not be neglected, especially when the film thickness is less than 1 μm. The estimation of the effective conductivity k_e most often presents a limited interest as it does not allow the contact resistances to be distinguished separately.

* Corresponding author. Fax: +33-2-40-68-31-41.

E-mail address: stephane.orain@isitem.univ-nantes.fr (S. Orain).

0017-9310/01/$ - see front matter © 2001 Published by Elsevier Science Ltd.
PII: S0017-9310(01)00025-4

Nomenclature

a	thermal diffusivity
b	thermal effusivity
C	product of heat capacity with density and layer thickness
c_p	specific heat
e	film thickness
k	thermal conductivity
n_g	number of generations performed by the GA
n_s	population size used with the GA
n_p	number of parameters
N_i	number of observations (per experiment and over time)
p	Laplace variable
Q	short pulse energy
r	correlation coefficient
R	film thermal resistance
R_{mf}	metal/film contact resistance
R_{fs}	film/substrate contact resistance
S	least squares function (°C^2)
t	time
T	temperature
T_i	initial temperature
V	voltage
X	sensitivity coefficient (dimensionless)
$\mathbf{X}$	sensitivity matrix

Greek symbols

β	parameter to be estimated
$\boldsymbol{\beta}$	parameter vector
Δ	variation
θ	temperature difference
ρ	density
τ	time constant

Superscripts

+	normalized/dimensionless
$\sim$	experimental

Subscripts

a	apparent
e	effective
m	metal
max	maximum
r	reference
s	substrate

An estimation procedure adapted to the thermal characterization of thin films is presented herein. It allows the simultaneous estimation of the thermal conductivity k and the contact resistances R_{mf} and R_{fs}. Because these parameters are highly correlated, a genetic algorithm (GA) is applied as the estimation procedure. Indeed, correlation among simultaneously estimated parameters can be a limiting factor of commonly used gradient-based estimation methods. By imitating genetic and selection mechanisms of nature, GAs are a non-gradient technique and thus, are not limited by a high correlation (provided the parameters are not a 100% correlated). The parameters are estimated by minimizing a least squares objective function containing calculated and measured temperatures.

In the following, the principle of the experimental technique, a photo-thermal technique, is given and, the mathematical model is described. Next, the fundamentals behind GAs are presented and the algorithm used is briefly discussed. The methodology of the sensitivity study performed prior applying the estimation procedure is then outlined. The final sections include first, the demonstration of the necessity to estimate the thermal resistance R_{mf}, followed by the results and conclusions from application of the GA to the thermal characterization of ZrO_2 thin films of different thickness. More particularly, the GA performance is compared with those obtained from application of both a common gradient-based method and a parametric study.

2. Description of the experimental technique

2.1. Principle

A measurement technique has been set up which allows the determination of the thermal conductivity of dielectric thin films. This technique belongs to the class of photo-thermal techniques and is briefly described in the following. A detailed description can be found in our previous studies [5–7].

A metallic layer is deposited on the dielectric thin film. The layer surface is irradiated by a laser short pulse of duration seven nanoseconds and incident energy $Q = 0.25$ J cm^{-2}. The metal layer is used as a temperature sensor by connecting it to one branch of a Wheatstone bridge. An increase in the metal temperature produces a voltage variation between two branches of the bridge, which is detected by a transient recording system (see Fig. 1). Calibration demonstrates that such a voltage variation is a linear function in temperature as shown in Eq. (2):

$$\Delta V = V(t) - V_i = K(T(t) - T_i), \tag{2}$$

where V_i and T_i, and $V(t)$ and $T(t)$ are the voltage and uniform temperature of the metal layer, initially and at time t, respectively, and K is a constant. A bridge balance is performed before irradiation to eliminate any effect of V_i, and thus, be sensitive to temperature variation only. Sensitivity to a few mV/K can be obtained.

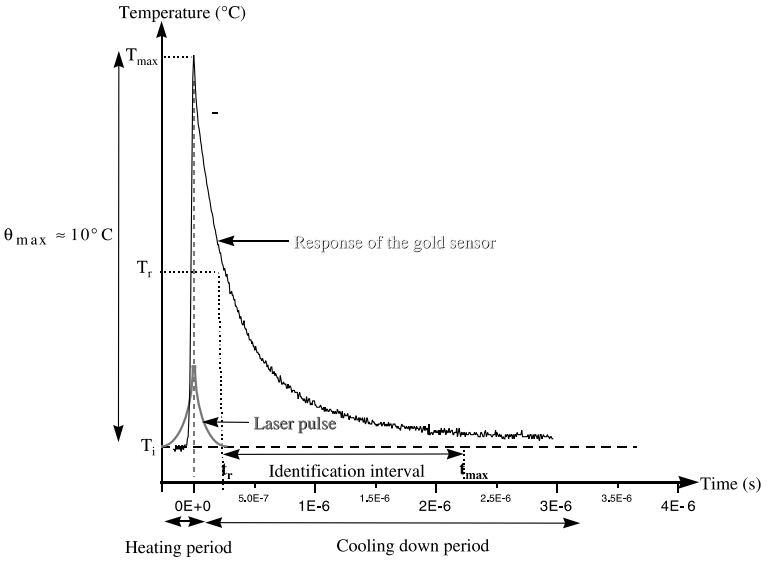

Fig. 1. Principle of the method.

The temperature $T(t)$ reaches a maximum $T_{\max}$ and then decreases during a cooling phase.

The parameters of interest are identified by minimizing the sum-of-squares error between calculated and experimental normalized temperatures during the cooling phase. The estimation procedure is performed over a temporal sequence (of ≈500 points) ranging from about 10^{-8} to 10^{-6} s. Temperatures are normalized ($^{+}$) according to:

$$\theta^{+} = \frac{\theta}{\theta_{\mathrm{r}}}, \tag{3}$$

where θ and θ_{r} are the temperature rises measured at time t and at a reference time t_{r}, respectively, as defined below:

$$\theta(t) = T(t) - T_{\mathrm{i}} \quad \text{and} \quad \theta_{\mathrm{r}}(t) = T(t = t_{\mathrm{r}}) - T_{\mathrm{i}}. \tag{4}$$

Normalization by θ_{r} ensures an analysis independent of the pulse energy Q absorbed by the metal sensor and avoids the determination of the constant K. The parameter t_{r} is chosen to maximize the sensitivity to the unknown parameters (see Effect of normalization). In practice, t_{r} is found to be about 2 μs. The genetic algorithm used as the estimation procedure is described in the next section.

2.2. Mathematical model

The mathematical model is formulated to express the temperature evolution in the metallic layer. The temperature field is assumed one-dimensional in the direction through the layers. The metallic layer is considered highly conductive compared to the dielectric substrate, and this latter is approximated as a semi-infinite body. This model is schematized in Fig. 2. The thermal properties are assumed constant in the temperature range investigated. Convection and radiation are neglected. The laser pulse is modeled as a dirac. All these simplifying assumptions lead to the expression of the Laplace transform of the metal temperature increase as a function of the layers thermal properties and their contact surface:

$$\begin{aligned}\bar{\theta} = Q(1 &+ \sqrt{(R/C)}b_{\mathrm{s}}th + p^{1/2}[R_{\mathrm{mf}}\sqrt{(C/R)}th \\ &+ b_{\mathrm{s}}(R_{\mathrm{mf}} + R_{\mathrm{fs}})] \\ &+ p[R_{\mathrm{mf}}R_{\mathrm{fs}}b_{\mathrm{s}}\sqrt{(C/R)}th])/(p^{1/2}[\sqrt{(C/R)}th + b_{\mathrm{s}}] \\ &+ p[C_{\mathrm{m}} + \sqrt{(C/R)}R_{\mathrm{fs}}b_{\mathrm{s}}th + C_{\mathrm{m}}\sqrt{(R/C)}b_{\mathrm{s}}th] \\ &+ p^{3/2}[C_{\mathrm{m}}R_{\mathrm{mf}}\sqrt{(C/R)}th + C_{\mathrm{m}}b_{\mathrm{s}}(R_{\mathrm{mf}} + R_{\mathrm{fs}})] \\ &+ p^{2}[C_{\mathrm{m}}R_{\mathrm{mf}}R_{\mathrm{fs}}b_{\mathrm{s}}\sqrt{(C/R)}th])\end{aligned} \tag{5}$$

and

$$\begin{aligned} th &= \tanh\left(\sqrt{pRC}\right), \\ R &= e/k, \\ C &= c_{\mathrm{p}}\rho e, \\ b_{\mathrm{s}} &= \sqrt{k_{\mathrm{s}}\rho_{\mathrm{s}}c_{\mathrm{p_s}}}, \end{aligned} \tag{6}$$

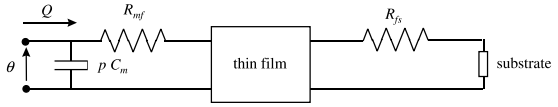

Fig. 2. Schematic of the mathematical model.

where p is the Laplace variable, b_s is the substrate effusivity and, c_p and ρ are heat capacity and density, respectively, whose values are taken identical to the values of the bulk materials. The substrate thickness and effusivity are known from other measurements. The original temperature θ is obtained after numerical inversion. The parameter vector β to be estimated include the thermal conductivity of the thin film k, and the two contact resistances R_{mf} and R_{fs}, that is $\beta = \{k, R_{mf}, R_{fs}\}$.

3. Description of the genetic algorithm

One method to simultaneously estimate all unknown parameters involves the minimization of an objective function, the sum-of-squares error S, with respect to the unknown parameters. In this work, the function S is defined by

$$S(\beta) = \sum_{i=1}^{N_i} \left[\theta_i^+(\beta, \tilde{t}) - \tilde{\theta}_i^+\right]^2, \tag{7}$$

where $\theta_i^+(\beta, \tilde{t})$ and $\tilde{\theta}_i^+$ are the calculated and measured normalized temperatures, respectively, and N_i is the number of measurements recorded over time. When the parameters are correlated or nearly correlated, the minimization of S using a common gradient-based method such as the Gauss linearization method becomes very difficult [8]. Indeed, in this case, gradient-directed searching mechanisms can show instabilities resulting in nonconvergence. Nongradient methods are then suggested to handle correlation problems. GAs are robust nongradient algorithms that belong to the field of evolutionary algorithms. They are neither bound to assumptions about the derivative of S nor require prerequisites such as initial guess values. These features makes them an excellent probabilistic search tool, which can be used with models that contain correlated parameters [9,10]. Because correlation exists among the three properties k, R_{mf}, R_{fs} in the mathematical model given in Eq. (6), application of a GA is well-adapted to the thermal characterization of thin films.

Like all evolutionary algorithms, GAs are based on the principles of biological evolution by imitating genetic and selection mechanisms of nature [11]. Each solution of the vector $\boldsymbol{\beta}$, also a potential minimum of the function S, is called an individual. Because the parameters are real in this study, floating-point representation is used; making an analogy with biological mechanisms, an individual is a chromosome with as many genes as there are unknown parameters, as illustrated in Fig. 3.

A GA generally starts by randomly generating an initial population of a large number of individuals (n_s) within the parametric search space (see POP_0 in Fig. 4). The individuals are then evaluated and ranked in terms of a fitness function, the function S in this study. Over

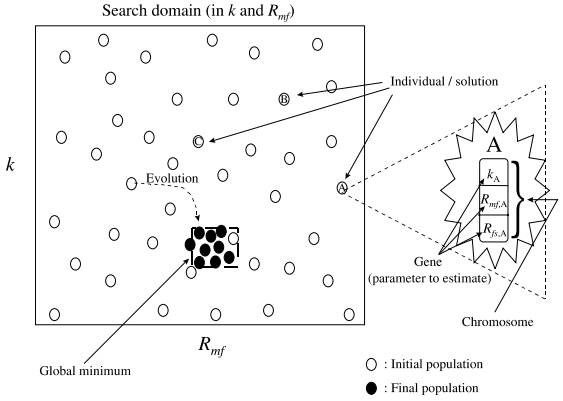

Fig. 3. GA functioning schematic.

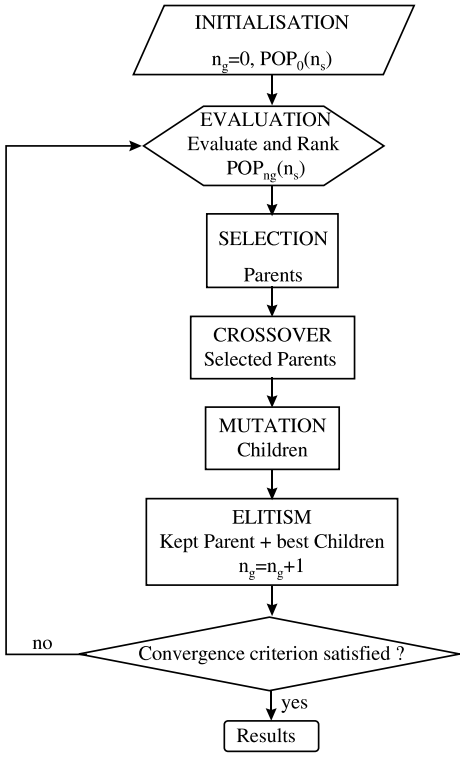

Fig. 4. Typical GA flowchart.

the course of several generations (n_g), the sequential application of the genetic operators *selection*, *crossover*, *mutation* and *elitism* makes the population evolve towards the region of the global minimum of S. A generation is accomplished when the sequence of genetic operators is applied to the individual parents. A typical GA flowchart appears in Fig. 4.

The selection operator determines the individual parents allowed to undergo crossover. The better the individuals are ranked, the higher their probability to be

selected. Crossover, which is the key exploration mechanism of GAs, is the crossing of a pair of chromosome parents to produce two chromosome children. The crossover probability set the number of parents which are simply cloned in the children generation. Mutation allows the changing of one or several genes of a chromosome children with a very small probability. The gene mutated can be replaced in a "global manner" with a random value (jump mutation) or in a "local manner" with the addition or subtraction of a small value to the gene (creep mutation). The mutation operator ensures that diversity of gene values is kept. Finally, the elitism operator is applied to keep the best solution(s) from one generation to the next.

In summary, the fundamental ways in what real GAs differentiate from gradient-based procedures are that they search from a population of solutions, not a single solution, they use payoff information (fitness function), not derivatives or other auxiliary knowledge, and they use probabilistic transition rules, not deterministic rules.

The genetic operators have all several variants. The variants employed in our GA follow the approach advised by Davis [12] which is to tailor the algorithm at hand. The GA scheme includes binary tournament selection and arithmetic crossover, both with probability 0.9, jump and creep mutations with probabilities equal to the inverse of the population size, and generational replacement with probability 0.9 for elitism. In-depth descriptions of these variants can be found in [10].

The GA produces as many generations as necessary until the convergence criterion defined by the user is reached. Because the mathematical model used for the thermal characterization of thin films is not time intensive, the criterion used in our GA is satisfied when first, 30 generations have been completed, and then, the best solution does not change, or roughly, during 30 generations. If convergence is not reached, the run stops when at most 200 generations have been completed. The absence of CPU time constraints also led us to choose a population size of 300 individuals, considered adequate for the simultaneous estimation of three parameters.

Due to the probabilistic nature of GAs, the determination of the global optimum requires a sufficient number of estimation runs. A GA efficiency thus consists of a balance between the search space definition and exploitation of the best solutions. As for any identification methods, approximate knowledge of the parameters to be estimated allows reduction of the number of runs to perform.

4. Sensitivity study

The aim of performing a sensitivity study before starting any estimation procedure is to evaluate the possibility to simultaneously estimate all unknown parameters. This depends on both magnitude of the parameters sensitivity coefficients and correlation among the parameters [8]. A sensitivity coefficient, X_i, is defined as the effect that a change in a particular parameter β has on the state variable, here the temperature θ:

$$X_i(t) = \beta_i \frac{\partial \theta(t)}{\partial \beta_i}, \tag{8}$$

X_i can be expressed in dimensionless form by

$$X_i^*(t) = \frac{\beta_i}{\theta^+_{\max}} \frac{\partial \theta^+(t)}{\partial \beta_i}. \tag{9}$$

The correlation coefficients are obtained by computing the off-diagonal elements of the correlation matrix. Assuming uncorrelated, additive, normally distributed errors with zero mean and constant variance, errorless independent variables and no prior information regarding the n_p parameters [8], the correlation coefficients can be approximated by

$$r_{ij} = \frac{P_{ij}}{\sqrt{P_{ii}P_{jj}}}, \quad i,j = 1, n_p \quad \text{and} \quad P = [\mathbf{X}^T\mathbf{X}]^{-1}, \tag{10}$$

where $\mathbf{X}$ is the sensitivity matrix.

In this study, the magnitude of both the sensitivity and correlation coefficients highly depends on the thin film thickness and thermal conductivity. The materials analyzed include dielectric films deposited with a thickness from 0.1 to 10 μm and having a thermal conductivity from 0.1 to 10 W m^{-1} K^{-1}. This sensitivity study has allowed the determination of

- which parameters could be simultaneously estimated depending on the dielectric film property values,
- the time interval during which k, R_{mf} and R_{fs} could be estimated, and,
- the reference time, giving the reference temperature used to normalize the temperature evolution so that sensitivity is maximized.

4.1. Sensitivity maximization and determination of the time interval for estimation

As a rule of thumb, estimation should be performed in the time interval where dimensionless sensitivity to all parameters is greater than 0.1 in magnitude. In the case the substrate is much more conductive than the film, Fig. 5 shows that the maximum of sensitivity to the thermal conductivity (X_k as defined in Eq. (8)) occurs around a time corresponding to the time constant of the system, τ, whose expression is approximated by

$$\tau \cong C_m(R_{mf} + R + R_{fs}) + \frac{e^2}{3a} + R_{fs}C, \tag{11}$$

where a is the film thermal diffusivity. The variable τ may take very different values depending on the

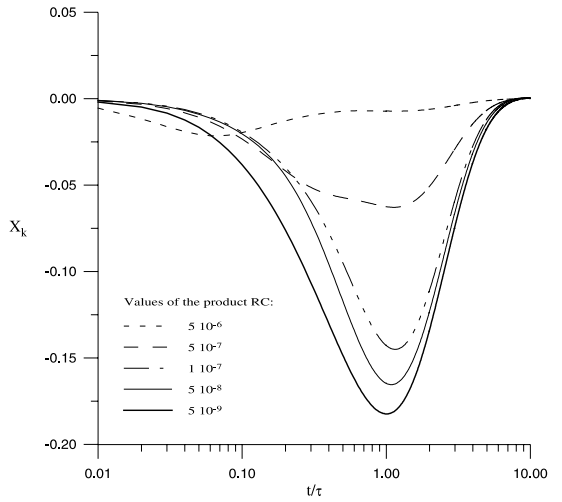

Fig. 5. Selection of the time interval that maximizes sensitivity to k.

materials nature and thickness: about 100 ns for a ceramic layer and up to several microseconds for a polymer. One can see on Fig. 5 that the time interval for which $X_k > 0.1$ takes place between $t = 0.2\tau$ and $t = 3\tau$.

One could also show that the maxima of sensitivity to R_{mf} and R_{fs} occur around the times τ_{mf} and τ_{fs}, respectively, equal to

$$\tau_{mf} = R_{mf} C_m \tag{12}$$

and

$$\tau_{fs} = R_{fs}(C_m + C). \tag{13}$$

In order to be able to simultaneously estimate the three parameters k, R_{mf} and R_{fs}, one has to select a time interval that includes the maxima of sensitivity to each. Fig. 6 shows the effect of both thermal conductivity and thickness of the film on the maximum of dimensionless sensitivity to R_{mf}, k and R_{fs}, in the case where R_{mf} and R_{fs} are set to 1×10^{-7} m^2 K W^{-1}. One can notice that the three sensitivity coefficients are about the same order of magnitude. Sensitivity to the metal/dielectric film contact resistance, R_{mf}, increases with the dielectric thermal conductivity but does not vary much with the film thickness. Measurement of the thermal conductivity is possible only if the material thermal resistance is larger than the contact resistances. Estimation of R_{fs} is possible only for a very small thickness. Finally, one can remark that the possibilities to simultaneously identify the three parameters correspond to a very few experimental conditions.

4.2. Effect of normalization

Normalization of the temperature evolution θ by a temperature θ_r taken at a time reference t_r highly effects the shape and magnitude of the sensitivity coefficients. With an aim to determining the time reference, it is convenient to look at the normalized sensitivity coefficient expressed by

$$X_i = X_i^0(t) - \frac{\theta}{\theta_r} \cdot X_i^0(t_r), \tag{14}$$

where X_i^0 is obtained using Eq. (8). Fig. 7 shows that X_i is a function of the ratio of the reference time over the characteristic time constant τ defined in Eq. (10). One can see that a reference temperature taken at a time greater than τ is adequate for normalization.

4.3. Correlation coefficient

Fig. 8 displays as a function of the film thickness and thermal conductivity the correlation coefficients $r(R_{mf}/k)$, $r(R_{mf}/R_{fs})$ and $r(k/R_{fs})$, corresponding to the degree of correlation between R_{mf} and k, R_{mf} and R_{fs} and k and R_{fs}, respectively. One can note that those coefficients are often larger than 0.9, value for which, as a rule of thumb, the parameters are considered correlated or nearly correlated and gradient-based methods show instabilities and failed to simultaneously estimate the parameters [8]. Fig. 8 shows that the correlation coefficient increases as the film thickness decreases. It is close to unity when the thickness is less than 100 nm. Indeed, for a small thickness, the metal temperature evolution can be approximated using

$$\vartheta \approx Q\left\{ \frac{1}{\sqrt{\pi t}} - \alpha \exp(\alpha^2 t) erfc(\alpha\sqrt{t}) \right\}, \tag{15}$$

where

$$\alpha = R_{mf} + R + R_{fs}\left(1 + \frac{C}{C_m}\right).$$

Eq. (15) confirms that for a small film thickness, R_{mf}, k and R_{fs} tend to be completely correlated. In other words, an infinity of solutions $\{k, R_{mf}, R_{fs}\}$ exists which leads to the same value of effective thermal resistance. In this case, the solutions given by the GA contain very different individual values but which provide the same value for the sum-of-squares error S.

The high degree of correlation existing between the film thermal conductivity and the film/substrate contact resistance makes the simultaneous estimation of these two properties very difficult. For this reason, it is convenient to introduce the notion of apparent thermal conductivity, k_a, which is characteristic of the temperature drop between the film and the substrate, and to simultaneously estimate k_a and R_{mf}. The apparent thermal conductivity is defined by

$$k_a^{-1} = k^{-1} + R_{fs} e^{-1}. \tag{16}$$

Unlike the effective conductivity, the apparent conductivity does not take into account the interfacial

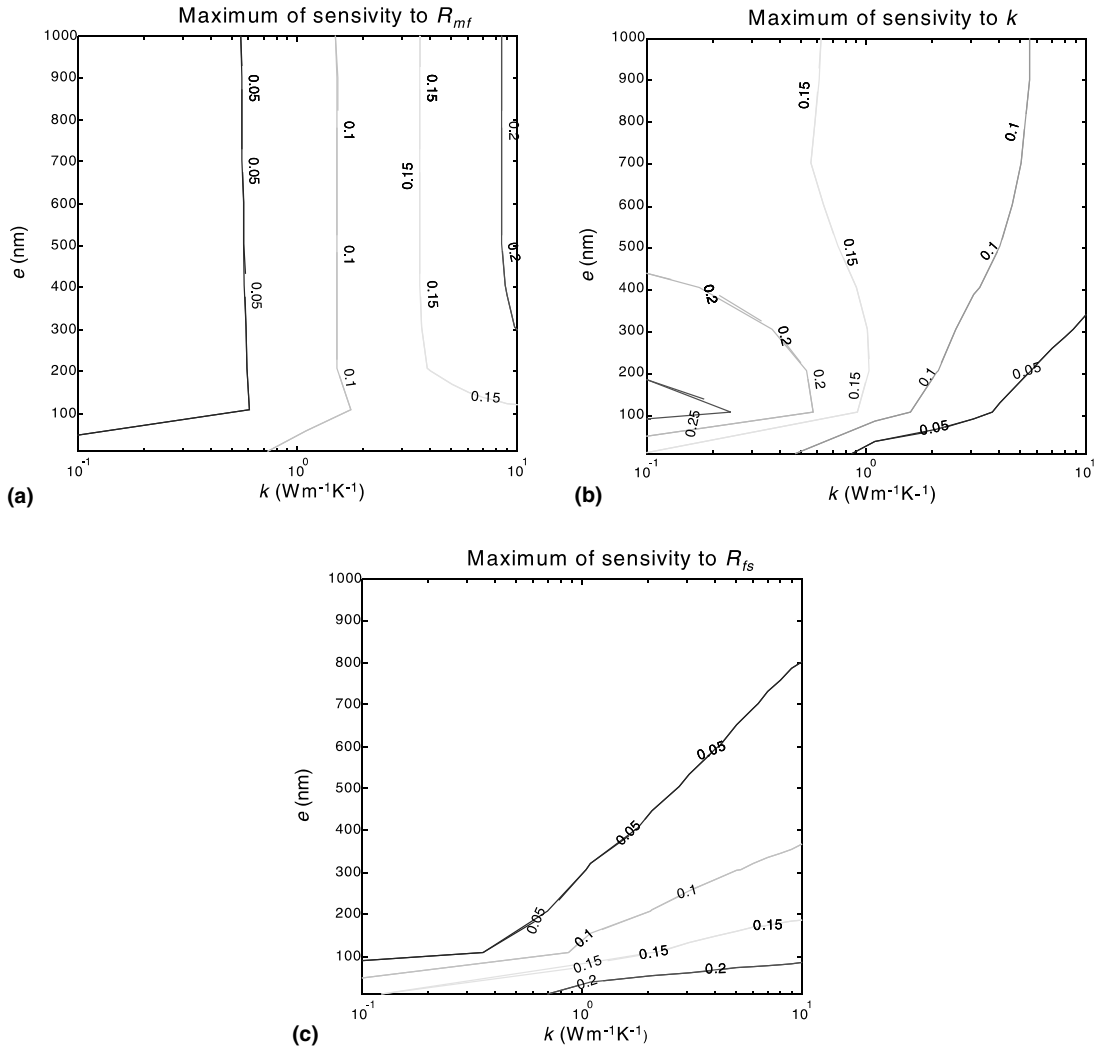

Fig. 6. Maximum of sensitivity to R_{mf}, k and R_{fs} vs. e and k.

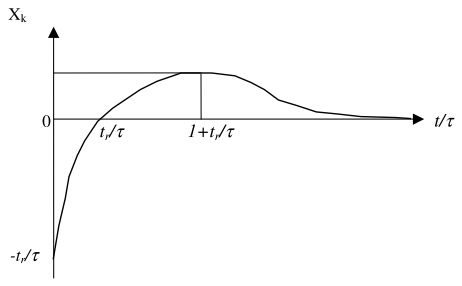

Fig. 7. X_k, vs. t/τ: determination of the reference time.

phenomena which are due to the sensor. Variations of k_a are therefore only the consequences to modification of the thin film structure which are related to modification of the elaboration process, the nature of the bulk materials, or the substrate rugosity.

4.4. Selection of the parameters to be estimated

This sensitivity study outlines that it is always possible to simultaneously estimate R_{mf} with a second parameter:

- k, if the film thickness is larger than 1 μm,
- k_a, if the film thickness is larger than 0.1 μm but less than 1 μm, and,
- R_{fs}, if the film thickness is less than 0.1 μm.

For a very small thickness ($e < 50$ nm), the parameters are completely correlated and thus, only the effective conductivity k_e can be estimated.

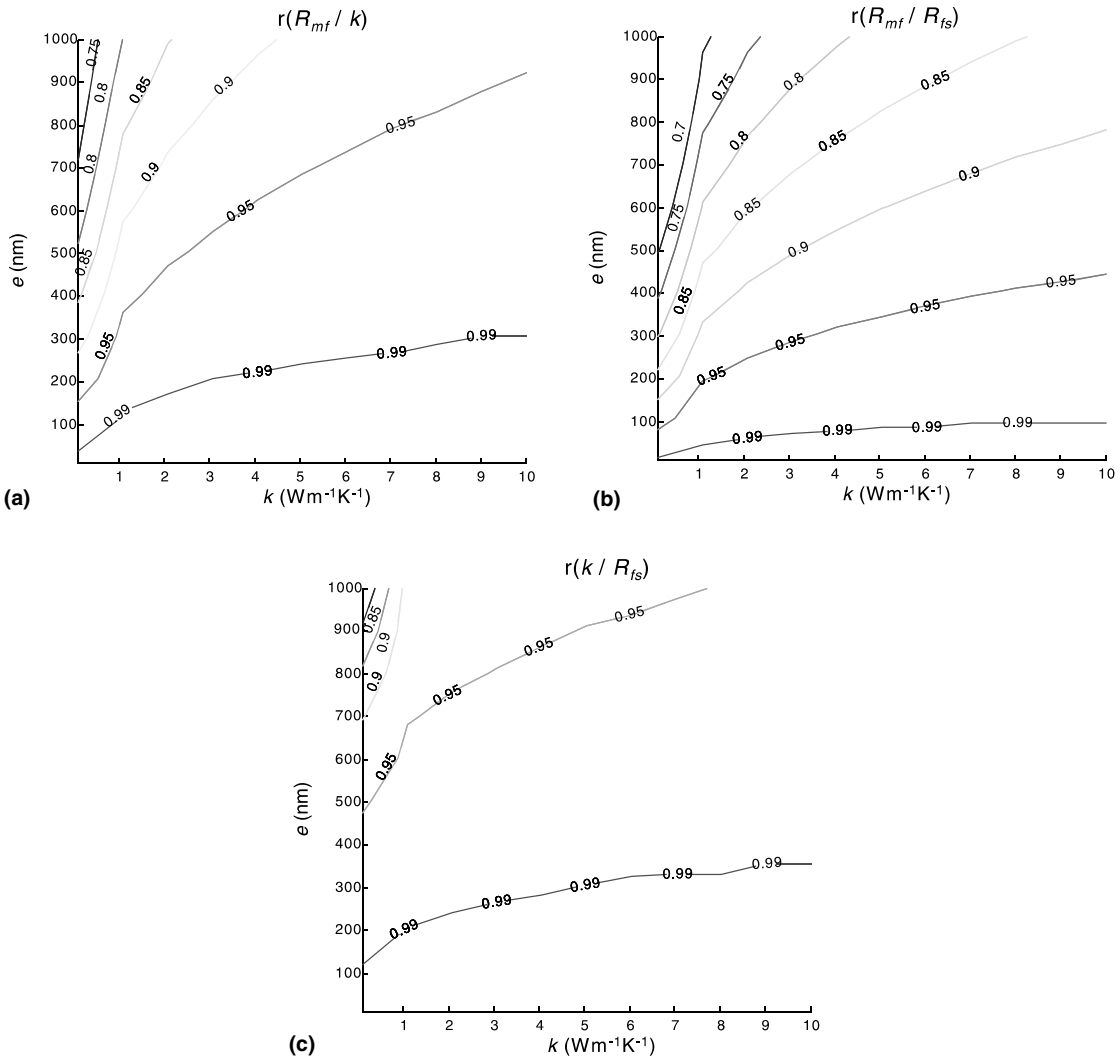

Fig. 8. Correlation coefficients $r(R_{mf}/k)$, $r(R_{mf}/R_{fs})$ and $r(k/R_{fs})$ vs e and k.

5. Results

First, the necessity to estimate the thermal contact resistance R_{mf} is shown. Then, the GA effectiveness and robustness is demonstrated using simulated data with very difficult estimation conditions which correspond to a large number of experimental conditions. Finally, the efficiencies of three estimation procedures, namely the GA, the Gauss method (gradient-based method) and the parametric study are compared using experimental data from ZrO_2 thin films of different thickness.

5.1. Necessity to estimate R_{mf}

When layering the metal sensor on a thick film ($e > 100$ μm), it has been shown that our experimental method allows the estimation of both the metal/film contact resistance, R_{mf}, and the film effusivity, b, [6]. The experimental results presented in Table 1 were obtained using the Gauss method as the two parameters R_{mf} and b are not correlated in thick film conditions.

On one hand, this investigation points out of the effect on R_{mf} of both the sensor and the substrate nature and, of the layering process. One can also notice that the effusivity values are comparable to the property values of the bulk material. On the other hand, this investigation stresses the high dependence of R_{mf} on the metal thickness: R_{mf} is 3.5 larger when the metal thickness varies from 200 to 350 nm, as illustrated on Fig. 9. This phenomenon is due to the thermal stress undergone during the evaporation in vacuum conditions. The thermal stress is proportional to the metal layering time.

Table 1
Effect of the layering technique and the metal and substrate nature on the contact resistance R_{mf}

Layering technique Metal/thick film	Radiofrequency		Evaporation	
	Cu/Al_2O_3	Cu/SiO_2	Au/Al_2O_3	Au/SiO_2
R_{mf} (m^2 K W^{-1})	8×10^{-8}	1.5×10^{-7}	1×10^{-7}	2×10^{-7}
b (J m^{-1} K^{-1} $s^{-0.5}$)	9700	5820	9500	5450

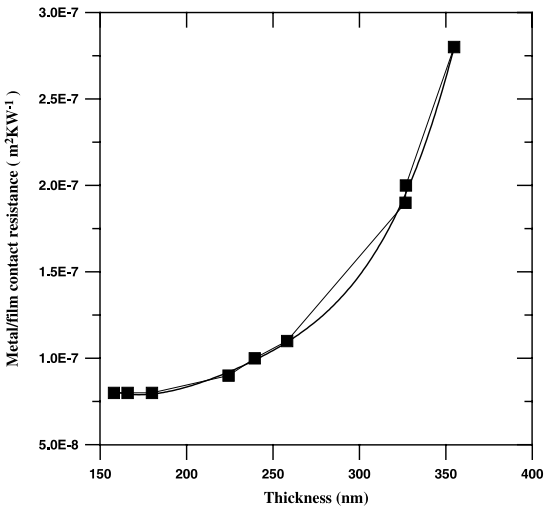

Fig. 9. Effect of internal stresses on the contact resistance R_{mf}.

One can realize that several parameters may effect the value of R_{mf} and therefore, it is crucial to estimate this property simultaneously with the thermal conductivity if one wants to study the thermal phenomena which take place inside the film.

5.2. Simulation results and GA performance

The simulated data consist of first generating exact temperatures using the analytical model given in Eq. (6) with the parameters k, R_{mf}, and R_{fs} set to true values provided in Table 2. Then, uniform random errors of standard deviation equal to 4% of the maximum temperature are added to these exact data. The parameter vector $\boldsymbol{\beta} = \{k, R_{mf}, R_{fs}\}$ is thought to be estimated for three different film thickness. The initial GA population is generated in a large domain, that is $k \in [0.01, 1000\ \mathrm{W\ m^{-2}\,K^{-1}}]$ and R_{mf} and $R_{fs} \in [10^{-15}, 10^{-5}\ \mathrm{m^2\ K\ W^{-1}}]$.

The performance of the GA was evaluated by averaging five runs, each realized with a different initial population, and calculating the means of each parameter and of the maximum sensitivities and correlation coefficients. The results shown in Table 2 clearly indicate that the GA allows the simultaneous estimation of highly correlated parameters. As one would expect, the estimation procedure is more accurate as the sensitivity coefficients are high, as outlined on Fig. 10. These simulated tests confirm the sensitivity study. One can also see that the small magnitude of the sensitivity coefficient of one parameter implies neither a bias on the estimation of the other parameters, nor algorithm instabilities.

5.3. Comparison of three estimation procedures using experimental data

The experimental results presented here were obtained from the analysis of ZrO_2 thin films of different thickness deposited on alumna substrate. This experimental study allows the testing of the efficiency and

Table 2
Results from simulation using GA

Thin film thickness	Parameters	True values	Estimates	Error (%)[a]	Maximum sensitivity	Correlation coefficient
$e = 10,000$ nm	R_{mf} (m^2 K W^{-1})	1×10^{-7}	1.05×10^{-7}	4.8	0.15	$r(R_{mf}/k) = 0.81$
	k (W m^{-1} K^{-1})	10	9.56	4.4	0.16	$r(k/R_{fs}) = 0.70$
	R_{fs} (m^2 K W^{-1})	1×10^{-7}	1×10^{-8}	90	0.02	$r(R_{mf}/R_{fs}) = 0.63$
$e = 500$ nm	R_{mf} (m^2 K W^{-1})	2.5×10^{-7}	2.57×10^{-7}	2.8	0.21	$r(R_{mf}/k) = 0.91$
	k (W m^{-1} K^{-1})	3	3.03	1.0	0.34	$r(k/R_{fs}) = 0.99$
	R_{fs} (m^2 K W^{-1})	1×10^{-7}	1.08×10^{-8}	8	0.10	$r(R_{mf}/R_{fs}) = 0.95$
$e = 100$ nm	R_{mf} (m^2 K W^{-1})	8×10^{-8}	7.80×10^{-8}	2.5	0.19	$r(R_{mf}/k) = 0.90$
	k (W m^{-1} K^{-1})	5	6.58	31.6	0.08	$r(k/R_{fs}) = 0.85$
	R_{fs} (m^2 K W^{-1})	3×10^{-7}	2.95×10^{-8}	1.67	0.29	$r(R_{mf}/R_{fs}) = 0.92$

[a] Percentage error between estimate and true value.

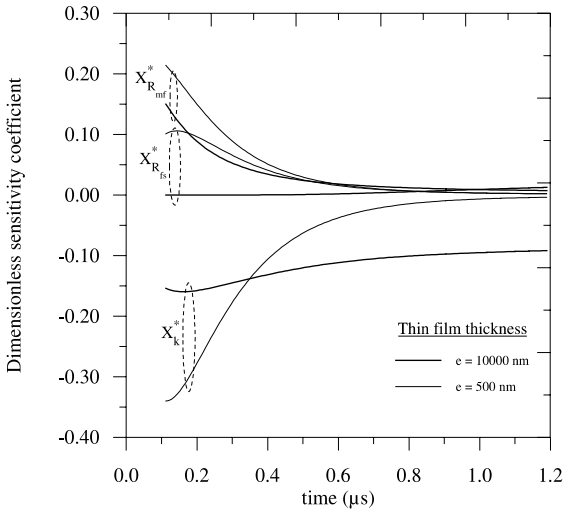

Fig. 10. $X^*_{R_{mf}}$, X^*_k, $X^*_{R_{fs}}$ for two film thicknesses (estimate values given in Table 2).

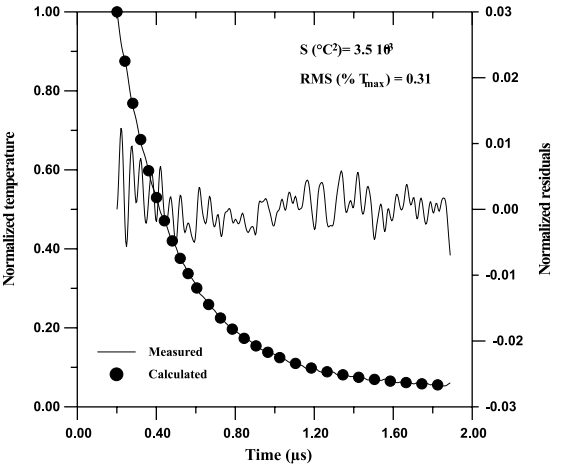

Fig. 11. Normalized residuals and temperature (ZrO_2 thickness $e = 166.6$ nm).

accuracy of three estimation procedures based on very different principles: the parametric study based on iso-S curves analysis, the Gauss method based on the gradient computation with no regularization [8] and, GAs, based on probabilistic rules. The fundamental behind the two first methods are briefly explained in the following. Results from application of these three methods can be found in Table 3.

The *parametric study* consists of determining the minimum of the sum-of-squares function S using, for instance, graphical representation. This type of estimation procedure only provides approximate values and the risk of error is high, mainly because of the risk to converge to a local minimum. This method becomes tedious and time intensive for the estimation of more than two parameters.

The *Gauss method* is very efficient to simultaneously estimate R_{mf} and$k$ when the film thickness is greater than 1 μm. For a smaller thickness, the correlation between the two properties is too high for the method to be stable and to converge without regularization. One can then identify k_a only (or R_{fs} only for $e = 166.6$ nm) by setting R_{mf} to its value estimated for a 2 μm-thick film. However, this setting introduces a bias for the estimation of k_a (or R_{fs}). Note that, in this comparative study, one chose the Gauss linearization method because it is an efficient estimation procedure which is easy to implement. However, it is possible that another gradient-based estimation procedure, for instance the Levenberg–Marquardt algorithm, could have been more efficient than the Gauss method for the problem investigated here.

The *genetic algorithm* allows the simultaneous estimation of the two unknown parameters even for very high degree of correlation. Furthermore, for 2000 nm-thick-film (case of no high correlation where $r(R_{mf}/k) = 0.85 < 0.9$), the GA finds values of R_{mf} and k comparable to those obtained with the Gauss method. Fig. 11 displays, in the case of a ZrO_2 thin film of

Table 3
Comparison of the results obtained from experimental data using the parametric study, the Gauss method and the GA

Thickness (nm)	Estimates	Correlation coefficient	Parametric study	Gauss	GA
2000	R_{mf} (m^2 K W^{-1})	0.85	1.0×10^{-7}	1.5×10^{-7}	1.6×10^{-7}
	k (W m^{-1} K^{-1})		2.00	2.25	2.30
1000	R_{mf} (m^2 K W^{-1})	0.91	1.5×10^{-7}	N/A[a]	2.0×10^{-7}
	k_a (W m^{-1} K^{-1})		1.50	1.70	1.67
250	R_{mf} (m^2 K W^{-1})	0.98	3.0×10^{-7}	N/A	2.5×10^{-7}
	k_a (W m^{-1} K^{-1})		1.00	0.90	0.96
166.6	R_{mf} (m^2 K W^{-1})	0.99	1.6×10^{-7}	N/A	1.4×10^{-7}
	R_{fs} (m^2 K W^{-1})		1.5×10^{-7}	1.3×10^{-7}	1.4×10^{-7}

[a] Not applicable.

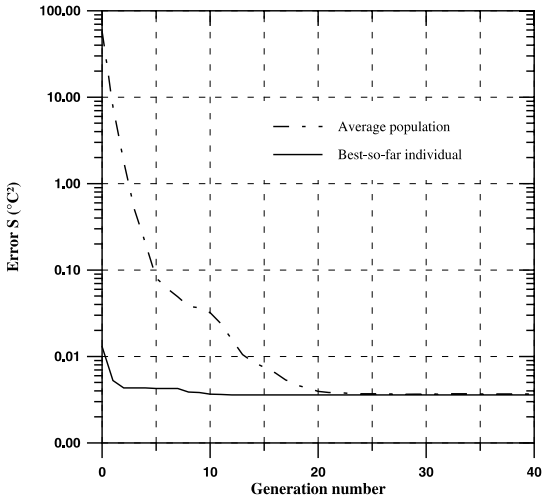

Fig. 12. Sum-of-squares error S evolution vs. generation number.

thickness 166.6 nm, the experimental and calculated normalized temperatures along with the residuals. The small values of both the sum-of-squares error ($S = 3.5 \times 10^{-3}$°C^2) and the root-mean-square error (RMS = 0.31% of the maximum temperature rise ΔT_{max}) highlight the excellent behavior of the estimation procedure. The correlation coefficient for that experiment is 0.992. The decrease of the function S over the generations is illustrated in Fig. 12 for both the best individual and the average population. The population and the best individual evolutions from the initial to the final generation shown in Fig. 13 stress the GA efficiency.

6. Conclusion

The estimation procedure presented in this paper allows the thermal characterization of thin films. It is based on genetic algorithms and exploits their non-gradient nature as a mechanism for the simultaneous estimation of correlated properties. GAs therefore overcome the main limitation of conventional simultaneous estimation techniques that depend on gradient information. The application of this procedure can be extended to the simultaneous estimation of a large number of parameters (i.e., >3).

The thermal properties of interest were the thin film thermal conductivity and the two contact resistances metal/film and film/substrate. A sensitivity study was performed to determine which parameters could be estimated depending on the film thickness and conductivity. The results using simulated data stressed the robustness and accuracy of the GA and, the results using experimental data obtained from the analysis of ZrO_2 thin films of different thickness deposited on alumna substrate showed the GA performance compared to the Gauss linearization method and the parametric study. Indeed, only the GA allowed the accurate simultaneous estimation of correlated parameters. Note that the GA scheme used in this work is by no means exhaustive and other GAs could be used.

The experimental results indicated that for films thicker than 1 μm, the film thermal conductivity is equivalent to the property value of the bulk material. Whereas for films less than 1 μm thick, a drop in the conductivity can be observed. This phenomenon can be explained by the important film/substrate contact resistance.

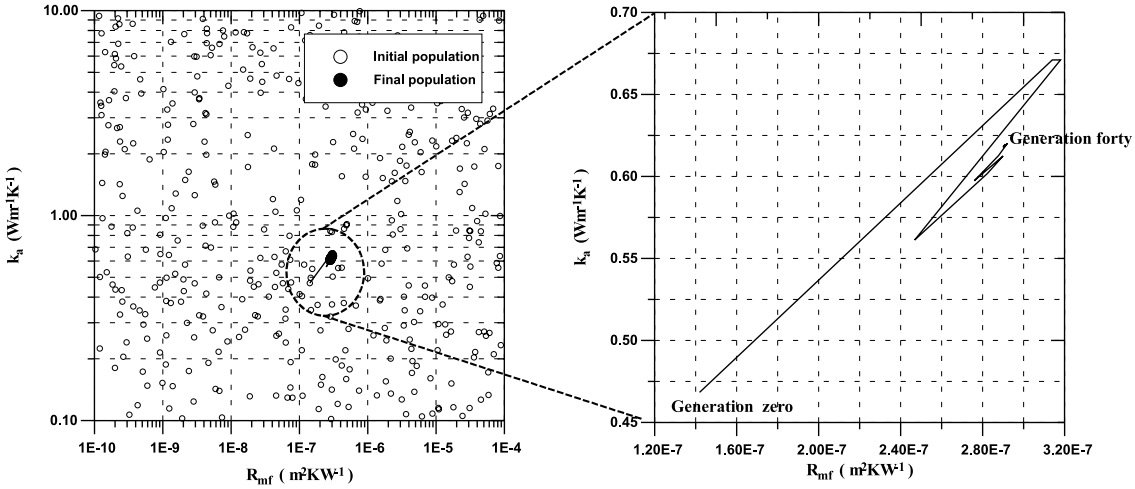

Fig. 13. Evolution of both the population (left) and the best-so-far individual (right).

Currently, experimental efforts are focused towards improving the metal/film contact resistance in order to improve the accuracy of the thermal conductivity estimation which is about 10%. These efforts are also expected to enable in some cases the simultaneous estimation of the three parameters of interest, the thermal conductivity and the contact resistances metal/film and film/substrate. Future work involves the analysis of the effect of both the film structure and microstructure on the parameters values.

References

[1] D.M. Bhusari, C.W. Teng, K.H. Chen, S.L. Wei, L.C. Chen, Traveling wave method for measurements of thermal conductivity of thin films, Rev. Sci. Instr. 68 (11) (1997) 4180–4183.

[2] F. Lepoutre, J. Lefevre, T. Lhermitte, L. Ainouch, P. Delpech, P. Forge, S. Hitschi, J.L. Joulaud, Mesures thermiques microscopiques, Int. J. Thermal Sci. 35 (1996) 344–354.

[3] S.M. Lee, D.G. Cahill, Heat transport in thin dielectric films, J. Appl. Phys. 81 (6) (1997) 2590–2595.

[4] J.C. Lambropoulos, Thermal conductivity of dielectric thin film, J. Appl. Phys. 66 (9) (1989) 4230–4242.

[5] S. Orain, Y. Scudeller, T. Brousse, Thermal conductivity of ZrO_2 thin films, Int. J. Thermal Sci. 39 (1999) 537–543.

[6] N. Hmina, Y. Scudeller, Thermal interface resistance and subsurface effusivity of submicronic metallic films on dielectric substrates: an experimental method for simultaneous determination, Int. J. Heat Mass Transfer 41 (1998) 2791–2798.

[7] S. Orain, Y. Scudeller, T. Brousse, N. Hmina, Détermination expérimentale de la conductivité thermique et de la capacité calorifique de films diélectriques submicroniques, Int. J. Heat Mass Transfer, submitted for publication.

[8] J.V. Beck, K.J. Arnold, Parameter Estimation in Engineering and Science, Wiley, New York, 1977 (Chapter 8).

[9] S. Garcia, J. Guynn, E.P. Scott, Use of genetic algorithms in thermal property estimation: part II - simultaneous estimation of thermal properties, Numer. Heat Transfer, Part A 33 (1998) 149–168.

[10] S. Garcia, Experimental design optimization and thermophysical parameter estimation of composite materials using genetic algorithms, Ph.D. Thesis, Department of Mechanical Engineering,Virginia Polytechnic Institute and State University, VA, Blacksburg, USA (Chapter 4)/Thèse de Doctorat, Laboratoire de Thermocinétique de l'ISITEM, Université de Nantes, France, June 1999.

[11] D.E. Goldberg, Genetic Algorithms in Search, Optimization and Machine Learning, Addison-Wesley, Reading, MA, 1989.

[12] L. Davis, Handbook of Genetic Algorithms. Part 1, Van Nostrand Reinhold, New York, 1991.